

Integrated Deep Learning Based Segmentation And Classification Method For Boundary Delineation Of Agricultural Fields In Multitemporal Satellite Images

Darsana K Gopidas

Ph.D. Research Scholar,

Department of Computer Science

darshanakgopidas@gmail.com

Sree Narayana Guru College, K KChavadi P.O

Bharathiar University, Coimbatore, Tamil Nadu, India.

Dr.R.Priya

Associate Professor & Head,

Department of Computer Science

priyaminerva@rediffmail.com

Sree Narayana Guru College, K KChavadi P.O

Bharathiar University, Coimbatore, Tamil Nadu, India.

Abstract

The multi-temporal satellite data gives the data in periodic basis which helps for continuous monitoring, but due to the earth's rotation, climatic changes, sensor characteristics, etc. There are too many distortions and noises which have to be removed before further processing for getting better results. In this study, a multispectral segmentation method for automated delineation of agricultural field boundaries in remotely sensed images is presented. In most image semantic segmentation tasks, the Deep Learning has shown its irreplaceable advantages, specifically the U-Net network architecture. With this motivation, in this work proposed a learning-based, simultaneous segmentation and classification method based on the Deep Multi-scale U-Net (DMU-Net) structure with deformable convolutional layers. In addition using cellular automata based Gaussian filtering is used to enhance the multitemporal images, to remove "noise" and to enhance the major direction. The second approach is linear feature extraction based on some parameters such as higher STD, length, strength and contrast. In this way, information from several spectral bands can be used for delineating field borders with different characteristics. Finally the experimental results reveal that the proposed segmentation method is more efficient than the existing segmentation techniques such as EGKL method and field boundary segmentation method in factors of each quantitative overall performance metrics and appropriateness for land-use classification.

1. Introduction

Agriculture is vital to the food security and economic growth for most countries in the world, especially in developing countries like India. Accurate information on field boundaries has considerable importance in precision agriculture and greatly assists land administration systems. The information obtained from field boundaries can provide valuable input for

agricultural applications like crop monitoring, yield prediction and land use classifications as provided by (Alemu2016).

According to European Commission (2018), agricultural areas refer to land suitable for agricultural practices, which include arable land, permanent cropland, and permanent grassland. Agricultural Field Boundaries (AFB) can be conceptualized as the natural disruptions that partition locations where a change of crop type occurs, or comparable crops naturally detach (North et al., 2018). Traditionally, AFB was established through surveying techniques, which are laborious, costly, and time-consuming. Currently, the availability of Very High Resolution (VHR) satellite imageries and the advancement in Deep Learning (DL)-based image analysis have shown potential for the automated delineation of agricultural field boundaries (Persello et al., 2019). However, their potential for the detection and delineation of agricultural boundaries have not been fully explored, they are limited to crop land classification (Belgiu and Csillik, 2018) and instance segmentation (Rieke, 2017).

Recently, Multi-resolution image segmentation techniques (Chen et al., 2015) and contour detection techniques such as Global Probabilities of Boundaries (GPB)(Arbeláez et al., 2011) are more recent techniques that can be applied to extract edges. Multi-Resolution Segmentation (MRS) is a region-margin segmentation technique, which merges pixels into uniform regions according to a homogeneity criterion. It stops when all possible merges exceed a predefined threshold for the homogeneity criterion. GPB combines multiscale spatial cues based on color, brightness, and texture with global image information to make predictions of boundary probabilities. Both approaches use spectral and spatial information in an unsupervised manner, so that they are designed to detect generic edges in an image. For this reason, those techniques cannot extract specific type of images edges (semantic contours), like AFB.

DL in image analysis is a collection of machine learning techniques based on algorithms that can learn features such as edges and curves from a given input image to address classification problems. Examples of Deep Learning methods used in remote sensing are Convolutional Neural Networks (CNNs) and Fully Convolution Networks (FCNs). CNNs and FCNs have been recently used for Land Cover and Land Use classification (LCLU). For instance, (Ajami et al., 2019), CNNs are applied to identify slums' degree of deprivation, considering different levels of deprivation including socio-economic aspects. FCN applications include detection of cadastral boundaries and delineation of agricultural fields in smallholder farms (Xia et al., 2019).

With this motivation, this work introduces a multi-task DCNN for AFB delineation using Multi-scale Convolutional to the U-Net architecture and develops the deformable U-Net and further named as Deep Multi-scale U-Net (DMU-Net) framework. This DMU-Net used to delineate agricultural field boundaries from satellite imagery images. Finally, field segments are obtained by adopting a combinatorial grouping algorithm exploiting the information of the segmentation hierarchy. This work addresses the delineation of the Agricultural Field Boundary (AFB) as a classification problem of class AFB boundary and non-boundary. The proposed diagram of delineation of boundary in agriculture field using DMU-Net is illustrated in Fig.1.

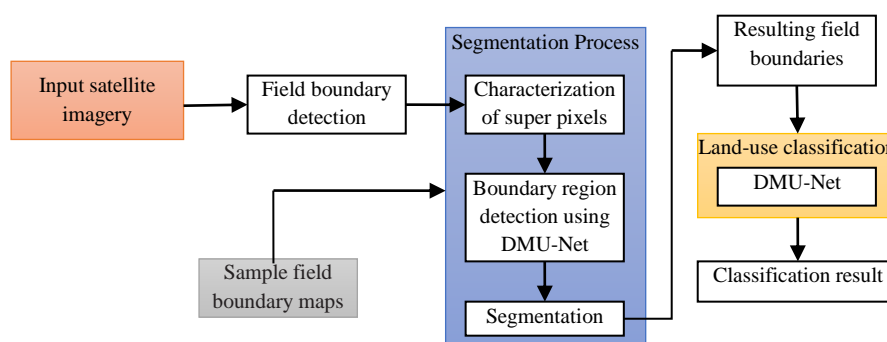


Fig.1.The proposed diagram of delineation of boundary in agriculture field using DMU-Net

The rest of this article is organized as follows. Section 2 describes the related work of boundary segmentation of agricultural field and section 3 describes the DMU-Net method with its main steps, presents the dataset and the experimental results. Finally, Section 4 closes with conclusions and future research.

2. Related Work

(García-Pedrero et al., 2018) proposed a new methodology based on a consensus of superpixel segmentations for delineating agricultural farm boundaries was presented. The most important contributions of this work have been to combine segmentation at different scales using superpixels and to incorporate information of the vegetative stage by means of images taken on different dates in order to obtain a single segmentation of the agricultural plots. Ghaffarian and (Turker2019) proposed a segmentation method based on active contour models for the automatic extraction of sub-boundaries (boundaries between different types of crops) within permanent agricultural fields. Active contour models used the results of both automatic fuzzy c-means clustering and edge detection to calculate an improved gradient vector flow (Zhu and Gao, 2016). This methodology is a promising solution for outlining sub-boundaries on agricultural plots with high intra-plot variability. However, to establish the geometry of agricultural fields, the authors used a reliable parcel database. (Xu et al., 2019) addressed the problem of outlining agricultural parcels using a stratified extraction method based on objects from RGB satellite imagery. According to the authors, the estimation of the segmentation scale based on spatial statistics can avoid sub-segmentation and over-segmentation to a certain degree. However, the accuracy of the segmentation and its subsequent analysis was limited in regions with complex objects. The aforementioned approaches have several drawbacks: they are sensitive to intra-plot variability, which can produce more segments than desired; and most of these methods rely heavily on a correct selection of parameters (e.g., the similarity measure used to group the pixels of the image), which requires prior knowledge of the scene or trial and-error tuning. In order to overcome these drawbacks, (García-Pedrero et al2017) proposed a methodology for delineating agricultural plots through agglomerative segmentation and other work of (Seiffert et al., 2010) using a machine learning method known as RUSBoost (Random Under Sampling and AdaBoost) classifier. This methodology used superpixels as minimum processing units, and a

superpixel agglomeration process where the decision to join two superpixels is taken by the classifier resulting in segmentation where agricultural plots are distinguished. A disadvantage is the amount of time taken to select the most suitable features to get a good performance from a machine learning classifier (Georganos et al., 2017). In addition, the variability in plot sizes and shapes means that certain configuration parameters do not allow for the proper delineation and classification of all agricultural plots in a scene (Im et al., 2014). (Liu and Lew 2016) used relaxed labels generated by bottom-up edges to guide the training process of Holistically-nested Edge Detector (HED). (Liu et al., 2017) proposed an edge detector that uses different image scales and aspect ratios to learn rich hierarchical representations, with an architecture that only adds 1×1 Convolutional layers to HED. The term nested is due to the inherited and progressively refined edge maps produced as side outputs, thus making successive edge maps more concise. The term holistic, despite not explicitly modelling the structured output, is because the network aims at training and predicting edges in an image-to-image fashion. More recently, (He et al., 2019) introduced a Bi-Directional Cascade Network (BCDN) structure to enforce each layer, which aims at focusing on a specific scale. However, Deep Learning techniques applied to agricultural field segmentation is a highly underexplored field of research. To enlighten some combined approaches, (Troya-Galvis et al., 2018) presented two proposals based on a multi-paradigm collaborative framework the first one is inspired by cascading techniques in machine learning, while the second one applies many collaborating one-vs.-all class extractors in parallel. (Csillik 2017) proposed to use a partition delivered by the simple linear iterative clustering superpixel algorithm as a starting segmentation point. (Gu et al., (2018) presented another approach composed of a minimum spanning tree algorithm for the initial segmentation, and the minimum heterogeneity rule algorithm for object merging in a fractal net evolution approach. Previous research on field boundary delineation from remote sensing data has mainly focussed on areas characterized by large plots using medium resolution images (Kamilaris and Prenafeta-Boldú, 2018). Automatic delineation of fields in smallholder farms is extremely challenging since boundaries are often not characterized by clearly visible edges, but need to be extracted by detecting changes in the textural and spectral patterns of different cultivations. The workflow combined Richer Convolutional Features(RCF)(Liu et al., 2017) and U-Net (Ronneberger et al., 2015) models respectively to detect soft edges (rivers and roads) and to detect regions such as hard edges and types of farmland while the work is difficult to replicate due to the lack of information provided in the methodology, the results showed a promising future for DL-based techniques. (Persello et al., 2019) proposed a strategy to detect field boundaries using a Fully Convolutional Network (FCN) in combination with a grouping algorithm. Field boundary detection was defined as a supervised pixel classification problem, using the SegNet architecture (Badrinarayanan et al., 2017) to distinguish boundary from non-boundary pixels. Although the importance of DL is increasing, there are significant challenges that have to be tackled to develop robust models. One of the most important drawbacks and barriers to the use of DL methodologies in agriculture is the lack of large labelled data sets needed for modelling. Because of this, it is possible to say that DL-based strategies for the generation of agricultural cadastres present a gap between laboratory-scale developments and their application in the real world. In order to

reduce the gap described above, in this work explored the use of a DL methodology for the automated mapping of agricultural boundaries over a large area with a heterogeneous landscape in agriculture field.

3. Proposed Methodology

The proposed methodology is based on a DCNN model, known as DMU-Net, to delineation of agricultural boundaries automatically. The main contributions are:

- The introduction of an automated technique based on a DMU-Net and combinatorial grouping to delineate agricultural fields in GIS images;
- The introduction of the boundary-based precision-recall accuracy assessment framework in remote sensing, which tolerates small localisation errors in the detected boundaries.

3.1. Study areas and available data

The full area of our main test site, illustrated in Fig. 2, is the Mid-Canterbury plains, South Island, New Zealand, an area of pastoral dairy farming (usually irrigated), sheep and beef farming (usually dry land), and arable cropping. Land use is dynamic, with significant farm conversion over the past 10 to 20 years—mostly to dairy farms. This conversion often involves wholesale removal of existing fences and hedges, installation of large pivot irrigators, and new field layouts. Cropping farms have dynamic crop rotations; with a wide variety of seed, grain, and vegetable crops grown (some fields will have several different crops per year). The high degree of land-use and seasonal change has led us to carry out two land-use classifications per year, one centred on a date in summer and a second around a date in winter. Each classification uses a time series of satellite data, typically starting 12 months before and continuing 9 months after the classification date. During this period a time series of some 15 to 19 images may be available. The land-use classifications of the area in Fig. 2 (dated 2010–12) included images from Landsat-5 and -7, and SPOT-4 and -5, and also use imagery from Sentinel-2A and -2B for current classifications. Fig. 2 shows one of the summer land-use classification results that use our field boundary map as input. To keep up with changes in field layouts, usually generate a new field boundary map for each classification date, using images from the same period as those used in the classification.

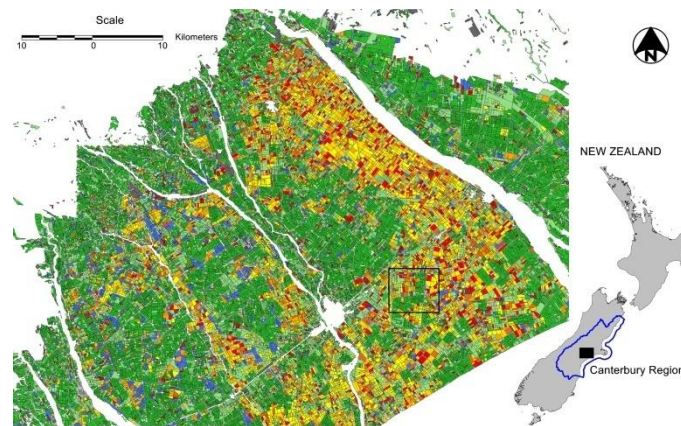


Fig. 2. The summer land-use classification results and study site on Mid-Canterbury plains, South Island, New Zealand (North et al., 2018), showing one of the land-use classification results that use our field boundary maps as input. Rivers, urban centres', and other non-agricultural areas have been masked out (white).

3.2. Field boundary detection with a deep multiscale CNN

The proposed boundary detection strategy takes advantage of the recent success of Deep MultiscaleCNN (DMCNN) for target classification (Chen et al., 2016). This section formulates the field boundary detection as a supervised target image classification problem to distinguish “boundary” from “non-boundary” pixels, respectively. The classification algorithm is trained to specifically detect field boundaries, therefore performing semantic edge detection. To this aim, adopt the deformable U-Net architecture (Jin et al., 2019), accommodates geometric variations in the images by learning and applying adaptive receptive fields driven by data, in contrast to standard DCNNs where the receptive field is constant. Therefore, it can be more robust to the spatial variations of the boundaries. This makes the deformable U-Net encoder significantly smaller and easier to train. The decoder is used to map the low-resolution feature maps learned by the encoder to the full resolution of the input image. Instead of using deconvolution or transposed convolutions, the decoder of deformable U-Net uses pooling indices computed in the corresponding max-pooling layers of the encoder to perform non-linear up sampling. The obtained up sampled maps are sparse and are then convolved with trainable convolutional filters to produce dense feature maps. This procedure eliminates the need for learning to up sample, reducing the number of trainable parameters and improving the accuracy of boundary delineation. The abovementioned characteristics make DMCNN with deformable U-Net (DMU-net) well suited for the considered boundary delineation problem as shown in Fig.3.

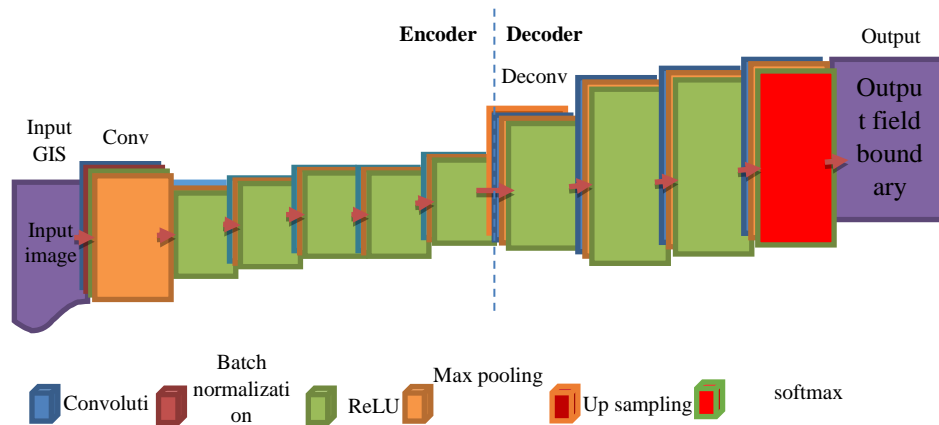


Fig.3.The architecture of DMU-Net

According to formula (1), the output size of the DMCNN model can be guaranteed to be consistent with the input image data size by using zero padding: where and are on behalf of the input and output images' size in DMCNN, respectively. F represents the convolution kernel with size 3×3 . P denotes the fill size with 1×1 .

$$I_{output} = \frac{I_{input} - CK + 2F}{S + 1}$$

Where I_{input} and I_{output} are on behalf of the input and output images' size in DMCNN, respectively. CK represents the convolution kernel with size 3×3 , F denotes the fill size with 1×1 and $S = 1$ stands for step size in this work. At the end of the proposed Deformable U-Net model in this work, skilfully adopted a convolution layer (whose size is 1×1) to lessen the number of feature graphs to 1. The final output will be disposed by the sigmoid function. It can obtain the value of each pixel between 0 and 1. Through the above processing, the final image is considered as the probability graph of DMCNN. The value corresponding to each pixel indicates the probability that the point belongs to the lesion.

Proposed Deformable U-Net

In Multi-scale Deformable U-Net, the network also regularizes the spatial contextual features and refines the exact location of the AFB by operating additional series of convolutions by using the probability of the boundary from the first prediction. The additional convolutional layers learn the contextual features from label space of the boundaries, and hence they filter the noise and increase the capability to detect more accurately the location of the contours, especially in the proximity of the corners. Train the network for 300 epochs using the Adam (adaptive moment estimation) optimizer that found more efficient and stable with respect to the choice of the hyper-parameters than the common Stochastic Gradient Descent (SGD). Since the "boundary" and "non-boundary" pixels are largely unbalanced, set the penalty for misclassifying the "boundary" class to be 10 times higher than for the "non-boundary". The architecture of the deformable U-Net is shown in Fig. 4.

It consists of an encoder path (left side) and a decoder path (right side) each with three layers. In the encoder path, each layer has two 3×3 deformable convolutions followed by a 2×2 max pooling operation with stride of 2, which doubles the number of channels and halves the resolution of input feature map for down-sampling. The encoder is followed by two 3×3 deformable convolutions called bottom layers. Each step in the decoder path contains a 3×3 deconvolution with stride 2 followed by two 3×3 deformable convolutions corresponding to its counterpart in the encoder except for the last layers where the label map is predicted. For the task of segmentation, the dimension of the last layer is $256 \times 256 \times 2$. For the classification with two cell types, the dimension should be $256 \times 256 \times 3$. The skip connection between encoder and decoder helps to preserve more contextual information for better boundary delineation segmentation.

Here, the modifications of the U-Net network are done that are mainly those two aspects. Firstly, residual network is introduced and second Batch normalization in the modified network. Residual network is to solve the problem of various errors and too much training time in deep network training. The most important one in the residual network is the residual module, which uses a method of fitting the residual map. It does not output the result of the convolutional layer directly, but the method of choosing the residual mapping, which call "shortcuts". Suppose that the network have a hidden layer named $H(x)$, and the hidden layer or a few of hidden layers satisfy $F(x) = H(x) - x$. Then combining such non-linear modules can get a fairly complicated network. To form a residual module, the residual network adds up the output of multiple convolutional layers and the initial input, which extracting the features of the image and reducing the training parameters in a way. And the residual network structure is relatively simple; it can also speed up training. To some extent, that solves the problem of network degradation in deep conditions. This residual module is a network implemented by a combination of neural networks and shortcut, where shortcut is equivalent to having a simple identity map with no extra parameters.

Residual network: In order to reduce the cost of computation, here improved the residual module (Constantin et al., 2018). Two 3×3 convolution layers were replaced with three convolution layers, where the sizes of the three convolution layers are 1×1 , 3×3 , and 1×1 . By replacing the residual module, the number of channels is reduced, and so does the amount of computation. On the other hand, the number of channels is reduced by the last 1×1 convolutional layer. To some extent, this ensures both accuracy and a reduction in computation.

Batch Normalization (BN): It is introduced to normalize the data. When using Stochastic Gradient Descent (SGD) for training, the activation function in the minibatch is calculated for normalization. After normalization, the mean of each dimension is 0 and the variance is 1. Batch Normalization scales the scale of each dimension in each level to the same. So it can use a relatively large learning rate when training, which will speed up the network training. When there is no BN layer, a smaller learning rate is needed when the promotion of the

accuracy is not obvious. However, the initial learning rate can be larger after BN being introduced. Because the convergence of the algorithm is relatively fast, the attenuation coefficient of the learning rate can also be larger. On the other hand, it solves the problem of gradient disappearance or gradient explosion in the process of back-propagation during training to some extent.

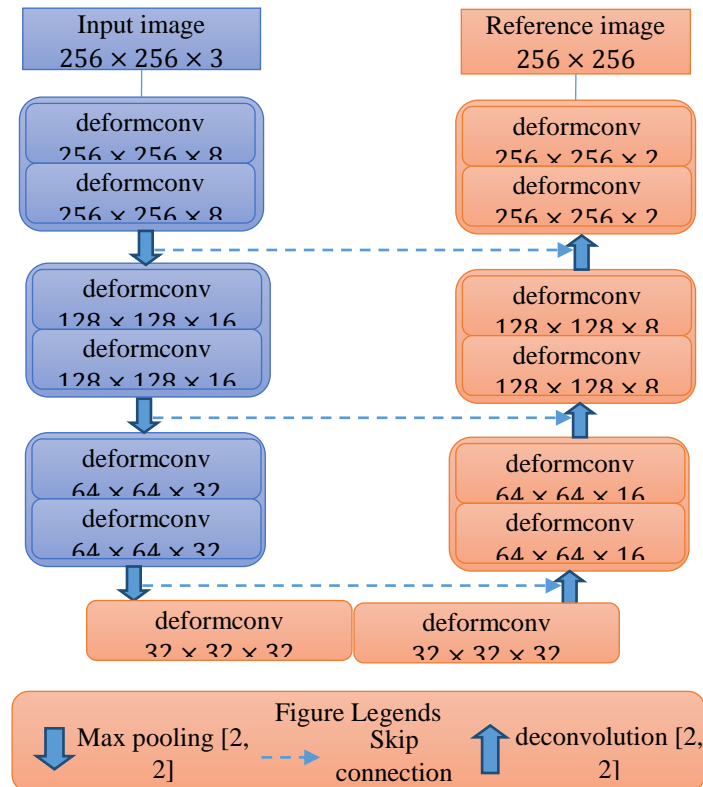


Fig.4. Architecture of the proposed deformable U-Net

Connecting boundaries and field segment generation: The delineation detector based on the deformable U-Net classification results in fragmented curves, which do not partition the image into closed segments. One can always recover closed contours from segmentation in the form of their boundary, but the reverse operation is not trivial. Applying the deformable U-Net to construct the finest set of regions, i.e., an over-segmentation from an oriented contour signal, to progressively merge the most similar adjacent regions by removing the weakest common boundary based on the average boundary strength. This process results in a hierarchy of regions that can be represented as GSI, a real-valued image obtained by weighting each boundary by its scale of disappearance. In this work, linearly combine the SGD detector with the deformable U-Netbased semantic edge detector.

4. Experimental results and discussion

The whole region of our main test vicinity is the mountains of mid-Canterbury, South Island, New Zealand, a location of pastoral dairy farming (normally irrigated), farm animals and cattle farming (commonly dryland) and agricultural property farming. Land use is dynamic, with widespread farm conversion over the past 10 to 20 years, normally to dairy farms. Now and again this conversion entails wholesale destruction of gift limitations and hedges, set up of large pivot irrigators, and new belongings layouts. It is used it on photograph datasets regular of those used for land-use scheduling to illustrate the segmentation method. Boundary

monitoring approach can be carried out to any optical photo. But, to selected pick most effective the larger spatial-resolution SPOT or sentinel-2 pixel (generally seven to nine images within the 21month duration) for ground boundary inspection from the images normally used for the land-use assessment level. The experiment compared the proposed DMU-Net performance to identify field boundaries against that of a conventional method such as EGKL with SVM(Priya et al., 2019) and field boundary with segmentation method (North et al., 2018)based on parameters such as Field boundary Extraction, overall accuracy, segmentation accuracy and processing time comparison.

Dataset description

This repository contains the RIT-18 dataset we built for the semantic segmentation of remote sensing imagery. It was collected with the Tetracam Micro-MCA6 multispectral imaging sensor flown on-board a DJI-S1000 octocopter. The main contributions of this dataset include 1) very-high resolution multispectral imagery from a drone, 2) six-spectral VNIR bands, and 3) 18 object classes (plus background) with a severely unbalanced class distribution. Figure 5 represents the input sensing onboard drone. The input has been converted into a grayscale image and represented in figure6

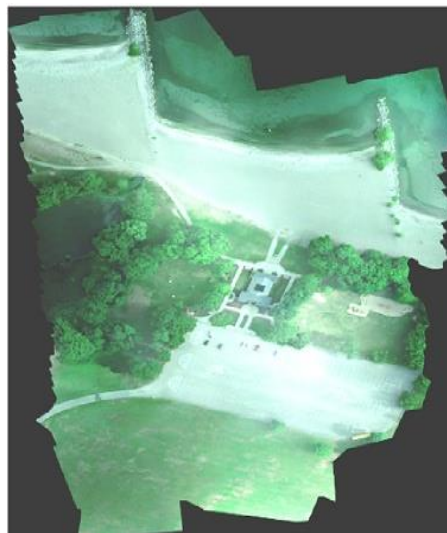


Fig 5 Input images



Fig 6 grayscale image

The pre-processing steps of image filtering have been used to remove the noise from the onboard drone image has been described in figure 7

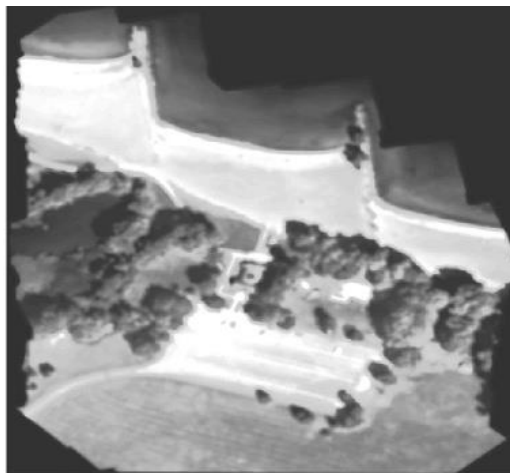


Fig 7 Filtered image

After the preprocessing steps, the image has been enhanced with the edge detection methods. the result of the work has been described in figure 8

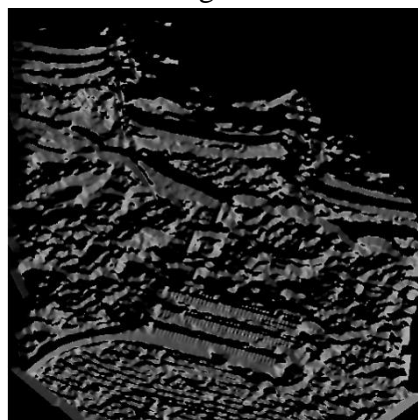


Fig 8 Edge detected image

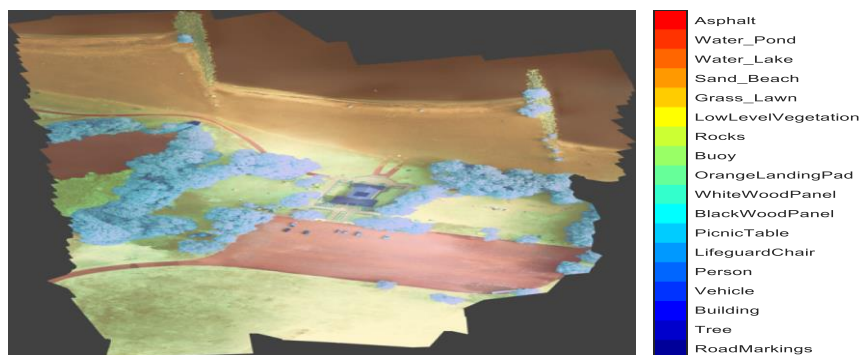


Fig 9 clustered output

Field boundary Extraction Accuracy (FEA)

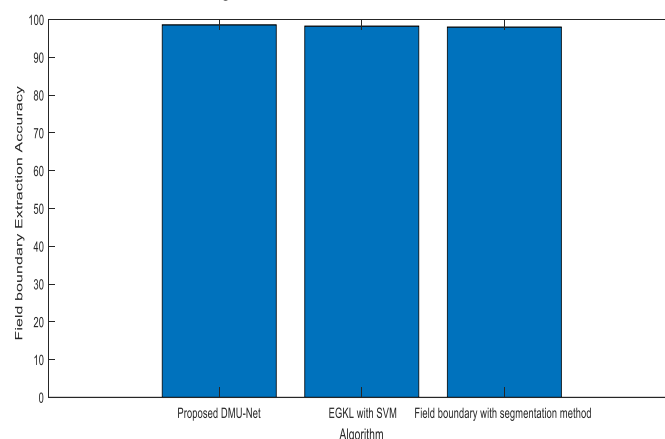


Fig.10.Field boundary Extraction Accuracy Results

The influence factors offer can be used for forfarmland) is the main factor that causes segmentation accuracy using the proposed misclassification in the farmland region. DMU-Net, which attains a high rate of Secondly, farmland in the urban region is not 98.59%. Firstly, the spectral similarity the dominant object and the low vegetation-between high vegetation-covered farmland covered farmland is often confused with and woodland (vegetation except construction land. The FEA values of existing EGKL with SVM and field boundary with segmentation are lower which is shown in Fig.10 with the rate of 98.25% and 98%. This indicates that the proposed stratified processing method is able to guarantee the thematic information extraction accuracy and the numerical results are given in Table.1.

Table1. Field Boundary Extraction Accuracy

Input	Proposed DMU-Net	EGKL with SVM	field boundary with segmentation

			method
Input imagery	98.59	98.25	98

Overall accuracy

Further examination of the classification performance of the proposed EGKL, existing segmentation tool and SPRING was conducted through the calculation of field boundary both raster and GIS. The fig.6 shows their comparable overall accuracy results and calculated as follows:

$$OA = \frac{TP + TN}{TP + TN + FN + FP}$$

Where True Positive Rate (TP) is the number of pixels that are correctly predicted as positive boundary, False Positive Rate (FP) is the number of pixels that are incorrectly predicted as positive boundary, True Negative Rate (TN) is the number of instances that are correctly predicted as negative boundary and False Negative Rate (FN) is the number of instances that are incorrectly predicted as negative boundary.

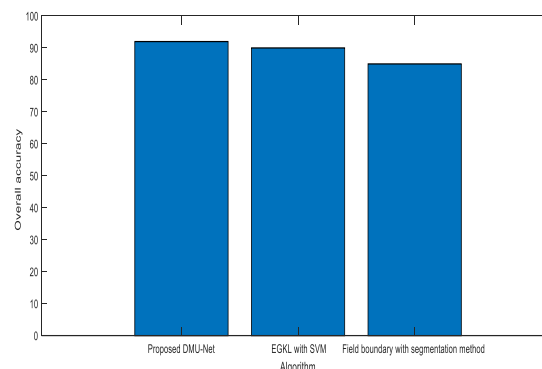


Fig.11.Overall Accuracy Results

From the fig.11 more accurate comparison between the segmentation approaches were clearly presented. The existing segmentation output generates many small polygons that require some form of filtering. This can be achieved by merging small zones into larger neighboring zones, which requires another layer of data analysis, and possibly expertise. At the same time the proposeddeformable U-Net requires no further processing the small polygon responses are included in the larger zone response when determining input rates. This advantage will lead the proposed DMU-Net method give high accuracy result 92% of boundary fields than the existing methods such as EGKL with SVM and field boundary with segmentation method with rate of 90% and 85% respectively. The numerical results of overall accuracy are given in Table 2.

Table2. Overall Accuracy Results

Input	Proposed DMU-Net	EGKL with SVM	Field boundary with
-------	------------------	---------------	---------------------

			segmentation method
Input imagery	92	90	85

Segmentation Accuracy

Two metrics are used to estimate the segmentation accuracy. The first metric is direct pixel count of the ground truth mask (manually segmented mask) and the segmented mask resulting from the segmentation algorithm. Let I_n be the number of non-zero pixels in the output nucleus. Let IM_n be the number of pixels in the manually segmented nucleus. The segmentation accuracy for the nucleus can be estimated by:

$$\text{segmentation accuracy} = \left[1 - \frac{IM_n - I_n}{IM_n} \right] * 100\%$$

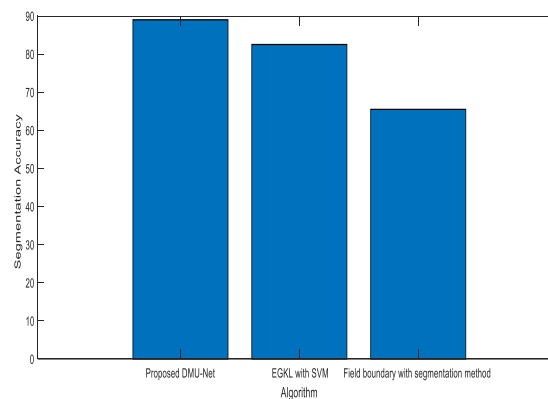


Fig.12.Segmentation Accuracy Results

From the Fig.12 the low segmentation accuracies were generally caused by the low resolution of the collected images in existing methods such as EGKL with SVM and field boundary with segmentation with rate of 82.52% and 65.5%. Such low-resolution effect can be noticed through comparing the achieved accuracies in three segmentation results. From the Fig.8 the proposed DMU-Net method is produce an effective segmentation accuracy result than the existing methods with rate of 89%. The numerical results of segmentation accuracy are given in Table 3.

Table 3. The numerical results of segmentation accuracy

Input	Proposed DMU-Net	EGKL with SVM	field boundary with segmentation method
Input imagery	89	82.52	65.5

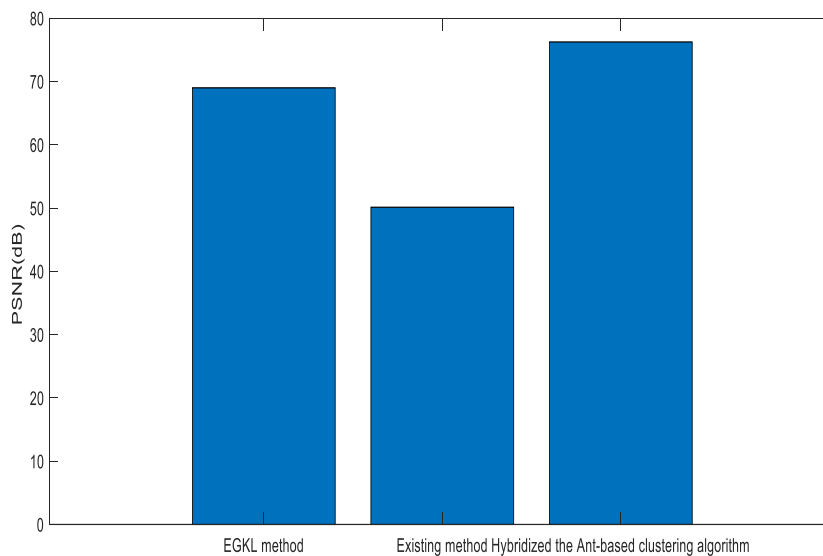


Fig.13. Result of PSNR

From the above Fig.13, the graph explains that the PSNR comparison for the number of segmentations of boundaries in multitemporal satellite images. From this graph it is learnt that the proposed segmentation using Hybridized the Ant-based clustering algorithm high PSNR rate of 76.24 dB than the previous methods such as EGKL with SVM and field boundary with segmentation with rate of 68.99dB and 50.12dB respectively. Thus the output explains that the proposed DMU-Net algorithm is greater to the existing algorithms in terms of better boundary delineation results for agricultural field. The numerical results of PSNR are given in Table 4.

Table 4. The numerical results of PSNR

Method	PSNR
EGKL method	68.99
Existing segmentation tool method	50.12

Processing Time comparison

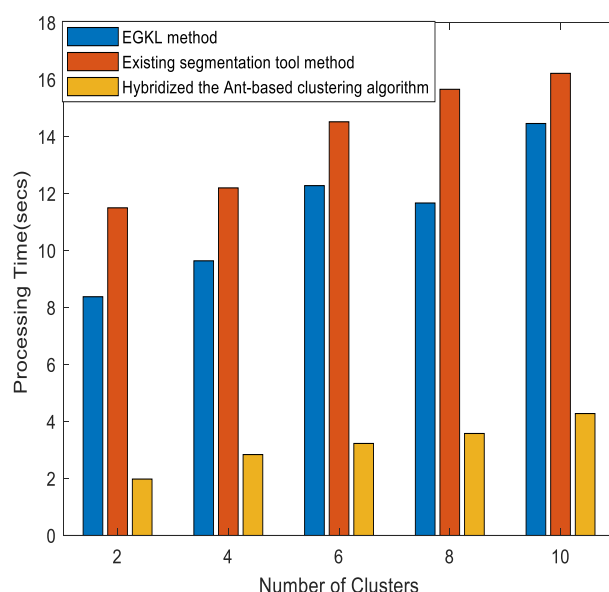


Fig.14. Result of Overall Processing Time

From the above Fig.14 the graph explains that the processing time comparison for the number of segmented regions in multitemporal satellite images. From this graph it is learnt that the proposed segmentation using Hybridized the Ant-based clustering algorithm provides lower processing time 4.28 than the previous methods such as EGKL with SVM and field boundary with segmentation with high rate of 14.46 and 16.22 respectively. Thus the output explains that the proposed DMU-Net algorithm is greater to the existing algorithms in terms of better boundary delineation results and for land use classification for agricultural field. The numerical results of processing time are given in Table 5.

Table 5. The numerical results of processing time comparison

Number of Clusters	2	4	6	8	10
EGKL method	8.38	9.64	12.28	11.67	14.46
Existing segmentation tool method	11.5	12.2	14.52	15.66	16.22
Hybridized the Ant-based clustering algorithm	1.98	2.84	3.23	3.58	4.28

5. Conclusion and future work

This work proposes boundary delineation technique based on a deep multiscale convolution network and a grouping algorithm to produce a segmentation delineating agricultural fields.

The experimental analysis conducted, using satellite imagery images acquired shows promising results. The proposed technique compares favourably against state-of-the-art boundary delineation detection algorithms in terms of the accuracy with rate of 92%. A visual inspection of the obtained segmentation results allows us to observe fairly accurate field delineations which are personalized to identify fields in an agricultural landscape with segmentation accuracy rate of 89%. These results show that the proposed automated field delineation method could facilitate the extraction of agriculture field boundaries framework are suitable for input into a land-use classification process. Future work should involve the investigation of developing new ways to improve the efficiency of Deep Learning training and inference by focusing on the many hyperparameters that are tuned to optimize the model's accuracy and resource usage by using swarm intelligence techniques. Because the performance of deep neural networks is highly sensitive to the choice of the hyperparameters that define the structure of the network and the learning process.

References

1. Alemu, M. M. (2016). Automated farm field delineation and crop row detection from satellite images. *Geo-Information Science and Earth Observation of the University of Twente*.
2. European Commission. *Cap Explained. Direct Payments for Farmers 2015-2020*; EU Publications: Brussels, Belgium, 2018.
3. North, H. C., Pairman, D., & Belliss, S. E. (2018). Boundary delineation of agricultural fields in multitemporal satellite imagery. *IEEE Journal of Selected Topics in Applied Earth Observations and Remote Sensing*, 12(1), 237-251.
4. Persello, C., Tolpekin, V. A., Bergado, J. R., & de By, R. A. (2019). Delineation of agricultural fields in smallholder farms from satellite images using fully convolutional networks and combinatorial grouping. *Remote sensing of environment*, 231, 111253.
5. Belgiu, M., & Csillik, O. (2018). Sentinel-2 cropland mapping using pixel-based and object-based time-weighted dynamic time warping analysis. *Remote sensing of environment*, 204, 509-523.
6. Rieke, Christoph. (2017). Deep Learning for Instance Segmentation of Agricultural Fields.
7. Chen, B.; Qiu, F.; Wu, B.; Du, H. Image segmentation based on constrained spectral variance difference and edge penalty. *Remote Sens.* **2015**, 7, 5980–6004.
8. Arbelaez, P., Maire, M., Fowlkes, C., & Malik, J. (2010). Contour detection and hierarchical image segmentation. *IEEE transactions on pattern analysis and machine intelligence*, 33(5), 898-916.
9. Ajami, A., Kuffer, M., Persello, C., & Pfeffer, K. (2019). Identifying a slums' degree of deprivation from VHR images using convolutional neural networks. *Remote sensing*, 11(11), 1282.
10. Xia, X., Persello, C., & Koeva, M. (2019). Deep fully convolutional networks for cadastral boundary detection from UAV images. *Remote sensing*, 11(14), 1725.

11. Garcia-Pedrero, A., Gonzalo-Martín, C., Lillo-Saavedra, M., & Rodríguez-Esparragón, D. (2018). The outlining of agricultural plots based on spatiotemporal consensus segmentation. *Remote Sensing*, 10(12), 1991.
12. Ghaffarian, S., & Turker, M. (2019). An improved cluster-based snake model for automatic agricultural field boundary extraction from high spatial resolution imagery. *International journal of remote sensing*, 40(4), 1217-1247.
13. Zhu, S., & Gao, R. (2016). A novel generalized gradient vector flow snake model using minimal surface and component-normalized method for medical image segmentation. *Biomedical Signal Processing and Control*, 26, 1-10.
14. Xu, L., Ming, D., Zhou, W., Bao, H., Chen, Y., & Ling, X. (2019). Farmland extraction from high spatial resolution remote sensing images based on stratified scale pre-estimation. *Remote Sensing*, 11(2), 108.
15. Garcia-Pedrero, A., Gonzalo-Martin, C., & Lillo-Saavedra, M. (2017). A machine learning approach for agricultural parcel delineation through agglomerative segmentation. *International journal of remote sensing*, 38(7), 1809-1819.
16. Seiffert, C., Khoshgoftaar, T. M., Van Hulse, J., & Napolitano, A. (2010). RUSBoost: A hybrid approach to alleviating class imbalance. *IEEE Transactions on Systems, Man, and Cybernetics-Part A: Systems and Humans*, 40(1), 185-197.
17. Georganos, S., Grippa, T., Vanhuysse, S., Lennert, M., Shimoni, M., Kalogirou, S., & Wolff, E. (2018). Less is more: Optimizing classification performance through feature selection in a very-high-resolution remote sensing object-based urban application. *GIScience & remote sensing*, 55(2), 221-242.
18. Im, J., Quackenbush, L. J., Li, M., & Fang, F. (2014). Optimum scale in object-based image analysis. *Scale Issues in Remote Sensing*, 197-214.
19. Liu, Y., & Lew, M. S. (2016). Learning relaxed deep supervision for better edge detection. In *Proceedings of the IEEE conference on computer vision and pattern recognition* (pp. 231-240).
20. Liu, Y., Cheng, M. M., Hu, X., Wang, K., & Bai, X. (2017). Richer convolutional features for edge detection. In *Proceedings of the IEEE conference on computer vision and pattern recognition* (pp. 3000-3009).
21. He, J., Zhang, S., Yang, M., Shan, Y., & Huang, T. (2019). Bi-directional cascade network for perceptual edge detection. In *Proceedings of the IEEE Conference on Computer Vision and Pattern Recognition* (pp. 3828-3837).
22. Troya-Galvis, A., Gançarski, P., & Berti-Équille, L. (2018). Remote sensing image analysis by aggregation of segmentation-classification collaborative agents. *Pattern Recognition*, 73, 259-274.
23. Csillik, O. (2017). Fast segmentation and classification of very high resolution remote sensing data using SLIC superpixels. *Remote Sensing*, 9(3), 243.
24. Gu, H., Han, Y., Yang, Y., Li, H., Liu, Z., Soergel, U., ...& Cui, S. (2018). An efficient parallel multi-scale segmentation method for remote sensing imagery. *Remote Sensing*, 10(4), 590.
25. Kamilaris, A., & Prenafeta-Boldú, F. X. (2018). A review of the use of convolutional neural networks in agriculture. *The Journal of Agricultural Science*, 156(3), 312-322.

26. Liu, Y., Cheng, M. M., Hu, X., Wang, K., & Bai, X. (2017). Richer convolutional features for edge detection. In *Proceedings of the IEEE conference on computer vision and pattern recognition* (pp. Ronneberger, O., Fischer, P., & Brox, T. (2015, October). U-net: Convolutional networks for biomedical image segmentation. In *International Conference on Medical image computing and computer-assisted intervention* (pp. 234-241). Springer, Cham.
27. Persello, C., Tolpekin, V. A., Bergado, J. R., & de By, R. A. (2019). Delineation of agricultural fields in smallholder farms from satellite images using fully convolutional networks and combinatorial grouping. *Remote sensing of environment*, 231, 111253.
28. Badrinarayanan, V., Kendall, A., & Cipolla, R. (2017). Segnet: A deep convolutional encoder-decoder architecture for image segmentation. *IEEE transactions on pattern analysis and machine intelligence*, 39(12), 2481-2495.
29. Chen, S., Wang, H., Xu, F., & Jin, Y. Q. (2016). Target classification using the deep convolutional networks for SAR images. *IEEE Transactions on Geoscience and Remote Sensing*, 54(8), 4806-4817.
30. Jin, Q., Meng, Z., Pham, T. D., Chen, Q., Wei, L., & Su, R. (2019). DUNet: A deformable network for retinal vessel segmentation. *Knowledge-Based Systems*, 178, 149-162.
31. Constantin, A., Ding, J. J., & Lee, Y. C. (2018, October). Accurate road detection from satellite images using modified u-net. In *2018 IEEE Asia Pacific Conference on Circuits and Systems (APCCAS)* (pp. 423-426). IEEE.
32. Priya R, DarsanaKGopidas, (2019). Automatic Boundary Delineation of Agricultural Fields in Multi temporal Satellite Imagery with Segmentation, *International Journal of Engineering and Advanced Technology (IJEAT)* ISSN: 2249 – 8958, Volume-9 Issue-2.
- 33.